

Error Rate Analysis for Bit-Loaded Coded MIMO-OFDM

Mohammad Mohammadnia-Avval, *Student Member, IEEE*, Chris Snow, and Lutz Lampe, *Senior Member, IEEE*

Abstract—Bit-loaded Orthogonal Frequency Division Multiplexing (OFDM) with convolutional coding is a powerful technique for transmission over quasi-static frequency-selective fading channels. Further enhancements in data rate are achieved by combining loaded OFDM with Multiple-Input Multiple-Output (MIMO) transmission. Motivated by the lack of appropriate error rate analysis techniques for this popular type of transmission system, in this paper we develop a novel analytical method for bit error rate (BER) and frame error rate (FER) estimation of bit-loaded coded OFDM and MIMO-OFDM systems using singular value decomposition (SVD), operating over frequency-selective quasi-static channels with non-ideal interleaving. Then, we introduce three different applications of the proposed analysis. First, we compare the performance of several OFDM bit-loading schemes and propose a hybrid loading scheme which selects the best loading for each channel realization from a number of candidates. Second, we introduce three adaptive interleaving schemes: (i) selecting the best interleaver from a number of predefined interleavers, (ii) a novel adaptive bit interleaving algorithm based on pairwise error probability, and (iii) a spatial interleaving scheme for MIMO-OFDM-SVD systems with separate information sources. Third, we introduce an adaptive coded modulation algorithm by using our BER and FER estimation technique.

Index Terms—Orthogonal frequency division multiplexing (OFDM), coding, bit-loading, error rate analysis, adaptive interleaving.

I. INTRODUCTION

Multicarrier communication systems based on Orthogonal Frequency Division Multiplexing (OFDM) have gained interest from the communications community in recent years, as evidenced by standards such as xDSL (digital subscriber lines), IEEE 802.11a/g for Wireless Local Area Networks (WLANs) [1], IEEE 802.16 (broadband wireless access), ECMA Multiband OFDM (MB-OFDM) for high-rate Ultra-Wideband (UWB) [2], and the 3GPP Long Term Evolution (LTE) wireless cellular systems. While OFDM accomplishes transmission in the temporal and spectral domains, Multiple-Input Multiple-Output (MIMO) technology exploits the spatial

domain by using multiple antennas at the transmitter and receiver. In general, the frequency-selective channel for these systems can be assumed to be very slowly time-varying relative to the transmission rate of the device, and can be approximated as quasi-static for the duration of one or more packet transmissions.

Given the frequency-selective quasi-static conditions present in many OFDM systems, it is beneficial to employ bit-loading algorithms to select non-identical modulation schemes for each OFDM subcarrier based on the channel conditions. Bit-loading techniques can be used for either (a) increasing the total throughput (by maximizing the sum data rate), or (b) decreasing the error probability or transmit power (by keeping the total rate fixed and adjusting the modulation per subcarrier in order to take advantage of those subcarriers with the best channel gains). In this work, we focus on the latter class of error rate minimizing loading schemes, of which a number of different algorithms exist [3]–[7].

In addition, most OFDM systems employ channel coding techniques such as bit-interleaved coded modulation (BICM) [8] with convolutional codes in order to mitigate the effects of the “fading” across OFDM subcarriers. Simulation-based approaches to obtain system performance in this setting are very time consuming due to the necessity of simulating the system over a large number of channel realizations. Thus, there is an interest in analytical methods for evaluating the performance of bit-loaded BICM-MIMO-OFDM operating over quasi-static frequency-selective fading channels. There are well-known techniques for bounding the performance of convolutionally-encoded transmission over many types of fading channels, e.g. [8], [9]. However, such classical bit error rate (BER) analysis techniques are not applicable to the OFDM systems mentioned above for several reasons. Firstly, the short-length channel-coded packet-based transmissions are non-ideally interleaved, which results in non-zero correlation between adjacent coded bits. Secondly, and more importantly, the quasi-static nature of the wireless channel limits the number of distinct channel gains to the (relatively small) number of OFDM subcarriers. This small number of distinct channel gains must not be approximated by the full fading distribution for a valid performance analysis, as would be the case in a fast-fading channel. Recent work has developed a pairwise error probability (PEP) analysis for loaded coded OFDM [10], [11]. However, the analysis in [10] assumes a uniform distribution of label and OFDM subcarrier positions for coded bits and the resultant expression [10, Ineq. (13)] is not amenable to numerical evaluation. The analysis in [11] is based on a Gaussian approximation [12] and we found

Copyright ©2010 IEEE. Personal use of this material is permitted. However, permission to use this material for any other purposes must be obtained from the IEEE by sending a request to pubs-permissions@ieee.org.

Manuscript received May 07, 2009; revised September 29 and December 17, 2009. This work was supported by the National Sciences and Engineering Research Council (NSERC) of Canada. The material in this paper was presented in part at the 2008 IEEE Wireless Communications and Networking Conference (WCNC '08).

Mohammad Mohammadnia-Avval and L. Lampe are with the Department of Electrical and Computer Engineering, University of British Columbia, Vancouver, BC, Canada. Chris Snow is with Research in Motion, Waterloo, ON, Canada. (e-mail: mohammadm@ece.ubc.ca, chsnow@rim.com, Lampe@ece.ubc.ca).

the resulting approximation of BER to be quite loose. As in [10], the effect of finite interleaving is not considered in the BER expression. A popular approach for adaptive loading and coding is the use of look-up tables with simulated performance results for coded transmission over the additive white Gaussian noise (AWGN) channel, based on which bit-loading and code rate selection is performed, e.g. [13], [14]. This approximative approach is not able to consider the effect of interleaving and also for this reason works well only for large numbers of OFDM subcarriers. In another line of work, e.g. [15], [16], the error rate for a hypothetical memoryless binary symmetric channel between encoder output and decoder input is considered, and it is argued that minimizing this error rate does also decrease the error rate of the actual coded transmission system. This approach does not take into account the properties of the applied channel code and, again, relies on the assumption of infinite interleaving.

In this paper, we develop a novel analysis technique for bit-loaded coded MIMO-OFDM systems (Section III), extending recent results for non-loaded coded single-input single-output (SISO) OFDM [17]. This method provides system designers with a simple way to study the performance of different bit-loading and channel coding schemes without resorting to lengthy simulations. We note that, as in e.g. [10], [13], [16], we assume identical transmit power in all OFDM subcarriers, which is necessary for systems such as UWB MB-OFDM where power spectral density is constrained. In Section IV we present three applications of the proposed analysis. First, we propose and evaluate a hybrid loading scheme which selects the best loading for each channel realization from a number of candidates. Second, we introduce three different adaptive interleaving algorithms. The first algorithm is based on selecting the best interleaver among a set of interleavers. In the second algorithm, a bit interleaver is designed based on the PEPs derived using our error rate estimation technique. Furthermore, for MIMO-OFDM systems employing singular value decomposition (SVD), we propose an adaptive space-frequency interleaving. The third application is an adaptive coded modulation scheme using our BER estimation technique. Numerical results confirming the accuracy of our error rate estimation and illustrating the applications mentioned above are shown in Section V for MB-OFDM and IEEE 802.11a/g systems, and also for the MIMO-SVD extension of IEEE 802.11a/g. While our work directly builds on the analysis method presented in [17], we note that we not only extend the performance analysis to the case of loaded OFDM and MIMO OFDM, but also introduce adaptive bit loading, interleaving, and coded modulation schemes. Part of this work, in particular the performance analysis for single-antenna loaded OFDM, has been presented in our conference publication [18].

Notation: In this paper, \mathbf{x} and \mathbf{X} denote a vector and a matrix, respectively. $[\cdot]^T$ and $[\cdot]^H$ denote vector transposition and matrix Hermitian, respectively, and $\text{diag}(\mathbf{x})$ denotes a matrix with the elements of \mathbf{x} on the main diagonal. \mathbb{C} denotes the field of complex numbers, \oplus denotes element-wise XOR, $\mathbb{E}\{\cdot\}$ is the expectation operator. Finally, \mathbf{I}_K denotes the identity matrix of size $K \times K$ and $Q(\cdot)$ is the Gaussian Q-

function [9].

II. SYSTEM MODEL

Before presenting the novel analysis and the improved designs, we first briefly establish the system model for coded bit-loaded MIMO-OFDM transmission.

A. Generic Model

Let us consider an N -subcarrier MIMO-OFDM system with N_T transmit and N_R receive antennas (we assume $N_T \leq N_R$). It employs a general bit-loading scheme, which selects a $2^{m_{i,j}}$ -ary quadrature amplitude modulation ($2^{m_{i,j}}$ -QAM) for subcarrier $1 \leq i \leq N$ over the antenna $1 \leq j \leq N_T$ based on the channel conditions.¹ For non-square constellations, we use the constellations proposed in [19]. We denote the average number of coded bits per modulated symbol by \bar{m} . The particular loading algorithms applied will be discussed in Section IV.

The system employs a (possibly punctured) convolutional code of rate R_c . We assume that the transmitter selects a vector of $L_b = R_c N \bar{m} N_T$ random message bits for transmission, denoted by

$$\mathbf{b} = [b_1 \ b_2 \ \dots \ b_{L_b}]^T. \quad (1)$$

The message bits are convolutionally encoded by the mapping

$$\mathcal{C} : \{0, 1\}^{L_b} \rightarrow \{0, 1\}^{L_c} \quad (2)$$

to produce the vector

$$\mathbf{c} = \mathcal{C}(\mathbf{b}) \quad (3)$$

of length $L_c = N \bar{m} N_T$. The vector \mathbf{c} is then interleaved by the mapping

$$\eta : \{0, 1\}^{L_c} \rightarrow \{0, 1\}^{L_c} \quad (4)$$

resulting in the vector

$$\mathbf{c}^\eta = \eta(\mathbf{c}) \quad (5)$$

of length L_c . The interleaved bits \mathbf{c}^η are finally modulated using $2^{m_{i,j}}$ -QAM on subcarrier $1 \leq i \leq N$ over antenna $1 \leq j \leq N_T$, where the modulation is represented by the mapping

$$\mathcal{M}_h : \{0, 1\}^{L_c} \rightarrow \mathbb{C}^{N N_T}. \quad (6)$$

Hence, the vector of the $N N_T$ modulated symbols is given by

$$\mathbf{x} = [x_{1,1} \ x_{1,2} \ \dots \ x_{1,N_T} \ x_{2,1} \ x_{2,2} \ \dots \ x_{2,N_T} \ \dots \ x_{N,1} \ x_{N,2} \ \dots \ x_{N,N_T}]^T = \mathcal{M}_h(\mathbf{c}^\eta), \quad (7)$$

where $x_{i,j}$ is the symbol on subcarrier $1 \leq i \leq N$ over antenna $1 \leq j \leq N_T$.

It is important to note the dependence of \mathcal{M}_h on the frequency-domain channel gains as a result of the channel gain dependent loading algorithms. For a particular channel gain, the mapping \mathcal{M}_h is obtained by running the chosen loading algorithm in order to select the modulation for each subcarrier.

¹With a slight abuse of notation, we use the term 2-QAM to denote binary phase shift keying (BPSK).

The channel gain for the i th subcarrier is given by the $N_R \times N_T$ matrix

$$\mathbf{H}_i = \begin{bmatrix} h_{1,1,i} & h_{1,2,i} & \cdots & h_{1,N_T,i} \\ h_{2,1,i} & h_{2,2,i} & \cdots & h_{2,N_T,i} \\ \vdots & \vdots & \ddots & \vdots \\ h_{N_R,1,i} & h_{N_R,2,i} & \cdots & h_{N_R,N_T,i} \end{bmatrix}, \quad (8)$$

where $h_{k,j,i}$ is the frequency-domain channel gain from transmit antenna j to receive antenna k for the i th subcarrier. Also we define the matrix \mathbf{D} as the block diagonal matrix of size $NN_R \times NN_T$ consisting of all \mathbf{H}_i matrices on the main diagonal.

We will assume that the MIMO-OFDM system is designed such that the cyclic prefix is longer than the channel impulse response and that timing and frequency synchronization have been established. Thus, we can equivalently consider the channel in the frequency domain and express the received symbols as

$$\mathbf{r} = \sqrt{\bar{E}_s} \mathbf{D} \mathbf{x} + \mathbf{n}, \quad (9)$$

where \mathbf{n} is a vector of independent complex AWGN variables of length NN_R with variance \mathcal{N}_0 and \bar{E}_s is the average received energy per modulated symbol assuming that $E\{\|\mathbf{D}\mathbf{x}\|^2\} = \mathbf{I}_{NN_R}$. The average received energy per information bit is $\bar{E}_b = \bar{E}_s / (R_c \bar{m})$.

The receiver employs a soft-output detector followed by deinterleaving, depuncturing, and Viterbi decoding, resulting in an estimate

$$\hat{\mathbf{b}} = [\hat{b}_1 \hat{b}_2 \dots \hat{b}_{L_b}]^T \quad (10)$$

of the original transmitted information bits.

While different MIMO processing strategies are possible and amenable to the framework proposed in Section III, for concreteness of the subsequent exposition we assume MIMO processing based on Singular Value Decomposition (SVD). Performing SVD on \mathbf{H}_i results in

$$\mathbf{H}_i = \mathbf{U}_i \mathbf{\Lambda}_i \mathbf{V}_i^H \quad (11)$$

where \mathbf{U}_i and \mathbf{V}_i are unitary matrices. The entries of the diagonal matrix $\mathbf{\Lambda}_i$ are non-negative singular values of \mathbf{H}_i : $\lambda_{i,1}, \lambda_{i,2} \dots \lambda_{i,N_T}$. In the standard SVD operation we have $\lambda_{i,1} \geq \lambda_{i,2} \geq \dots \geq \lambda_{i,N_T}$ and in MIMO-SVD transmission, \mathbf{V}_i is applied to the transmitted signal and \mathbf{U}_i^H is applied to the received signal. This will result in N_T parallel subcarriers with gains $\lambda_{i,j}$ for $1 \leq j \leq N_T$. Then we put these gains in a vector $\boldsymbol{\lambda}$ of length NN_T according to how encoded bits are assigned to different subcarriers. For convenience, we define the diagonal matrix $\mathbf{\Lambda} = \text{diag}(\boldsymbol{\lambda})$.

In the following, we describe two popular (practical) OFDM systems and channel models which we will consider in the performance evaluation in Section V.

B. MB-OFDM System and Channel Model

As the first example OFDM system, we have chosen MB-OFDM for high data-rate UWB [2], [20]. MB-OFDM uses 128 subcarriers and operates by hopping over 3 sub-bands (one hop per OFDM symbol) in a predetermined pattern. We will assume that hopping pattern 1 of [2] is used (i.e., the

sub-bands are hopped in order). As a result we can consider MB-OFDM as an equivalent 384 subcarrier OFDM system. After ignoring pilot, guard, and other reserved subcarriers, we have $N = 300$ data-carrying subcarriers.

Channel coding consists of classical BICM [8] with a punctured maximum free distance rate 1/3 constraint length 7 convolutional encoder and a multi-stage block-based interleaver (see [2] for details). In the standard, the interleaved coded bits are mapped to 4-QAM symbols using Gray labeling. To maintain the same data rates but decrease the error probability, we instead employ loading as described above with $\bar{m} = 2$ coded bits per subcarrier.

For a meaningful performance analysis of the MB-OFDM proposal, we consider the channel model developed by IEEE 802.15 for UWB systems [21]. The channel impulse response is based on a modified Saleh-Valenzuela model [22]. As well, the entire impulse response undergoes an ‘‘outer’’ lognormal shadowing. The channel impulse response is assumed time invariant during the transmission period of (at least) one packet (see [21] for detailed description). We consider the UWB channel parameter sets CM1 and CM3 [21].

C. IEEE 802.11a/g System and Channel Model

The second example system we consider is IEEE 802.11a/g, which employs 64 subcarriers, of which $N = 48$ are used for data transmission [1]. Channel coding is again BICM, with a punctured maximum free distance rate 1/2 constraint length 7 convolutional encoder. We adopt the quasi-static exponentially-decaying multipath Rayleigh fading model used in [10], [11], where the gain over subcarrier i from transmit antenna j to receive antenna k is given by

$$h_{k,j,i} = \sum_{\ell=0}^{L_m-1} \bar{h}_{k,j}(\ell) \exp\left(-j \frac{2\pi n \ell}{64}\right), \quad (12)$$

where L_m is the number of channel taps and $\bar{h}_{k,j}(i)$ is the i th component of the channel impulse response, modeled as a complex Gaussian random variable [10], [11]

$$\bar{h}_{k,j}(\ell) \sim \mathcal{CN}(0, \sigma_0 \exp(-\ell T_s / T_{\text{rms}})), \quad (13)$$

where

$$\sigma_0 = 1 - \exp(-T_s / T_{\text{rms}}), \quad (14)$$

$T_s = 50$ ns is the receiver sampling rate, and T_{rms} is the RMS delay spread of the channel.

We also consider the extension to this system when $N_T = 2$ antennas are used at the transmitter and $N_R = 2$ antennas are used at the receiver. As stated before, we use SVD for MIMO processing, but we note that our analysis would also be applicable to the spatial multiplexing or Alamouti coding as used in IEEE 802.11n.

III. BER ANALYSIS FOR CODED MIMO-OFDM WITH BIT-LOADING

We now present the method for approximating the performance of bit-loaded coded MIMO-OFDM systems operating over frequency-selective, quasi-static fading channels. This method is based on approximating the performance of the

system over individual channel realizations. Following the approach for non-bit-loaded SISO-OFDM in [17], we start by considering the set of error vectors for bit-loaded OFDM.

A. Set of Error Vectors

Consider a convolutional encoder initialized to the all-zero state, where the reference (correct) codeword is the all-zero codeword. We construct all L input sequences which cause an immediate deviation from the all-zero state (i.e., those whose first input bit is 1) and subsequently return the encoder to the all-zero state with an output Hamming weight of at most w_{\max} . Let \mathcal{E} be the set of all vectors e_ℓ ($1 \leq \ell \leq L$) representing the output sequences (after puncturing) associated with these input sequences, i.e., $\mathcal{E} = \{e_1, e_2, \dots, e_L\}$. Let l_ℓ be the length of e_ℓ (the number of output bits after puncturing), and let a_ℓ be the Hamming weight of the input associated with e_ℓ . Note that the choice of w_{\max} governs the value of L (i.e., once the maximum allowed Hamming weight is set, the number of error events L is known).

We term e_ℓ an ‘‘error vector’’ and \mathcal{E} the set of error vectors. The set \mathcal{E} contains all the low-weight error events, which are the most likely deviations in the trellis. As with standard union-bound techniques for convolutional codes [9], the low-weight terms will dominate the error probability. Hence, it is sufficient to choose a small w_{\max} . For example, the punctured MB-OFDM code of rate $R_c = 1/2$ [2] has a free distance of 9, and choosing $w_{\max} = 14$ (resulting in a set of $L = 242$ error vectors of maximum length $l = 60$) provides results which are not appreciably different from those obtained using larger w_{\max} values.

We note that in case of loading in OFDM, the combination of coding and modulation is not a linear operation, and thus the error-rate performance will depend on the transmitted codeword. Hence, it is not sufficient to consider only the all-zero word as reference codeword. Nevertheless, for tractability and simplicity of the analysis, we always choose one codeword (in which the message bits are randomly generated) as reference. Extensive simulations (see also Section V) have confirmed that the choice of the reference codeword is not critical.

B. Pairwise Error Probability

Next, we determine the PEP by considering error events starting in a given position i of the chosen reference codeword. The set ζ of allowable starting positions i has size $|\zeta| = R_c L_c$, and each element i of ζ is an index $1 \leq i \leq L_c$, which is code-dependent. For example, for a code of rate $R_c = 1/2$ the allowable starting positions are $\zeta = \{1, 3, 5, \dots, L_c - 1\}$.

We consider each error vector e_ℓ for $1 \leq \ell \leq L$, and form the full error codeword

$$\mathbf{q}_{i,\ell} = \underbrace{[0 \ 0 \ \dots \ 0]}_{i-1} \underbrace{e_\ell}_{l_\ell} \underbrace{[0 \ 0 \ \dots \ 0]}_{L_c - l_\ell - i + 1}^T \quad (15)$$

of length L_c by padding e_ℓ with zeros on both sides as indicated above. Given the error codeword $\mathbf{q}_{i,\ell}$ and given that codeword \mathbf{c} is transmitted, the competing codeword is given by

$$\mathbf{v}_{i,\ell} = \mathbf{c} \oplus \mathbf{q}_{i,\ell}. \quad (16)$$

Interleaving and modulation results in the vector of QAM symbols

$$\mathbf{z}_{i,\ell} = \mathcal{M}_{\mathbf{h}}(\mathbf{v}_{i,\ell}^\eta), \quad (17)$$

where $\mathbf{v}_{i,\ell}^\eta = \eta(\mathbf{v}_{i,\ell})$ is the interleaved version of $\mathbf{v}_{i,\ell}$.

The PEP for the ℓ th error vector starting in the i th position is then given by

$$\text{PEP}_{i,\ell}(\mathbf{\Lambda}) = Q \left(\sqrt{\frac{\bar{E}_s}{2\mathcal{N}_0} \|\mathbf{\Lambda}(\mathbf{x} - \mathbf{z}_{i,\ell})\|^2} \right). \quad (18)$$

Note that the PEP depends on the particular channel realization \mathbf{D} only through the matrix of singular values $\mathbf{\Lambda}$.

C. Performance Analysis

The PEP from (18) is now used to obtain an approximation of the BER for a particular matrix of channel gains $\mathbf{\Lambda}$, which we denote as $P(\mathbf{\Lambda})$. To this end, the bit error rate for the error event starting in a position $i \in \zeta$ ($1 \leq i \leq L_c$) and error vector $e_\ell \in \mathcal{E}$ ($1 \leq \ell \leq L$) is given by

$$P_{i,\ell}(\mathbf{\Lambda}) = a_\ell \cdot \text{PEP}_{i,\ell}(\mathbf{\Lambda}), \quad (19)$$

where a_ℓ is the number of information bit errors associated with e_ℓ . Summing over all L error vectors, we obtain an approximation of the BER for starting position i as

$$P_i(\mathbf{\Lambda}) = \sum_{\ell=1}^L a_\ell \cdot \text{PEP}_{i,\ell}(\mathbf{\Lambda}). \quad (20)$$

Since all allowable starting positions are equally likely, the BER $P(\mathbf{\Lambda})$ can be written as

$$P(\mathbf{\Lambda}) = \frac{1}{R_c L_c} \sum_{i \in \zeta} \min \left[\frac{1}{2}, \sum_{\ell=1}^L P_{i,\ell}(\mathbf{\Lambda}) \right], \quad (21)$$

where we tightened the union bound (20) by the maximum value of 1/2 before averaging over starting positions.

Finally, the average BER for a given number N_c of channel realizations, where the i th channel realization is denoted by $\mathbf{\Lambda}^{(i)}$ ($1 \leq i \leq N_c$), is given by

$$\bar{P} = \frac{1}{N_c} \sum_{i=1}^{N_c} P(\mathbf{\Lambda}^{(i)}). \quad (22)$$

Similarly, we can obtain the $X\%$ outage BER performance as

$$P_{\text{out}} = \max_{\mathbf{\Lambda}^{(i)} \in \mathbf{\Lambda}_{\text{in}}} P(\mathbf{\Lambda}^{(i)}). \quad (23)$$

where $(100 - X)\%$ best channel realizations are contained in $\mathbf{\Lambda}_{\text{in}}$. This provides information about the minimum performance that can be expected of the system given the $X\%$ outage rate.

In pseudocode, the algorithm to calculate $P(\mathbf{\Lambda})$ according to (21) is

```

Run loading algorithm to obtain  $\mathcal{M}_h$ 
 $P := 0$ 
for  $i \in \zeta$  do
   $P_i := 0$ 
  for  $\ell := 1$  to  $L$ 
    form  $\mathbf{q}_{i,\ell}$  as per (15)
    calculate  $\mathbf{v}_{i,\ell} = \mathbf{c} \oplus \mathbf{q}_{i,\ell}$  as per (16)
    form  $\mathbf{v}_{i,\ell}^\eta = \eta(\mathbf{v}_{i,\ell})$  using mapping (4)
    calculate  $\mathbf{z}_{i,\ell} = \mathcal{M}_h(\mathbf{v}_{i,\ell}^\eta)$  as per (17)
    calculate  $P_{i,\ell}$  as per (19)
     $P_i := P_i + P_{i,\ell}$ 
  endfor
   $P := P + \min(\frac{1}{2}, P_i)$ 
endfor
 $P := P/(R_c L_c)$ 

```

The PEP formula of (18) can also be used to obtain the approximate frame error rate (FER) for a specific channel realization $\mathbf{\Lambda}$, which we denote as $FER(\mathbf{\Lambda})$. First we derive the possibility of not having any error at position $i \in \zeta$ ($1 \leq i \leq L_c$) as

$$C_i(\mathbf{\Lambda}) = \max \left[0, 1 - \sum_{\ell=1}^L \text{PEP}_{i,\ell}(\mathbf{\Lambda}) \right]. \quad (24)$$

The FER is the probability of having at least one error in the frame, which can be related to $C_i(\mathbf{\Lambda})$ as follows

$$FER(\mathbf{\Lambda}) = 1 - \prod_{i \in \zeta} C_i(\mathbf{\Lambda}). \quad (25)$$

D. Computational Complexity

We note that the computational complexity of the analysis scales linearly with L (the size of the set of error vectors) and with L_c (the codeword length). Especially the choice of L allows to trade off complexity and accuracy (see also Section V-B). But even for large L , the analysis requires much fewer operations compared to the alternative of performing system simulations, especially for reasonably low error rates. To provide an appreciation of the run-time savings using the proposed method, we note that the analysis for $L \approx 250$ and $L_c = 600$ takes only a few seconds per channel realization on a modern PC, and the outage BER for a large number of channel realizations (e.g., $N_c = 500$) can be obtained in the time it would take to perform simulations for only one channel realization. Finally, we note that long packet lengths can be considered without any increase in complexity (if they are segmented into codewords of length L_c , as is usually the case in practical systems), since the error rate for each codeword will be identical as a result of the quasi-static channel conditions.

IV. BIT-LOADING, ADAPTIVE INTERLEAVING AND ADAPTIVE CODED MODULATION FOR MIMO-OFDM

In this section we present several different algorithms to accomplish high-performance adaptive coded MIMO-OFDM based on the analytical error-rate expressions derived in the previous section.

A. Bit-Loading Algorithm for Coded MIMO-OFDM

A plethora of bit-loading algorithms for OFDM systems have been proposed in the literature. Some examples of these are: the Hughes-Hartogs algorithm (HHA) [3], [4], the algorithm of Chow, Cioffi and Bingham (CCB) [5], the Piazzo algorithm [6], and the algorithm of Fischer and Huber [7]. The reader is referred to the respective papers for the details of each loading algorithm. Also, in [23], a new way of bit-loading was proposed. In this method, the loading algorithm is not performed for every channel realization; it is done only for one channel realization and the resulting bit-loading is just sorted for other channel realizations according to their subcarrier gains. Therefore, it is less complex than any other method. By using this method and using, for example, CCB as the primary loading algorithm, we have a bit-loading algorithm which we will refer to as sorted CCB.

All the mentioned algorithms have the same shortcoming: they do not guarantee that the selected loading is appropriate for coded OFDM, i.e., BICM-OFDM. The reason for this is that coding and interleaving have a great impact on the error-rate performance, but the above-mentioned algorithms do not consider them. Here, we propose a bit-loading algorithm for coded OFDM system which also considers the effects of coding and interleaving. In our algorithm, for each specific channel realization, interleaver, average rate, and transmit power, we compute the approximate performance of the system for a set of bit-loading algorithms and then the bit-loading with minimum BER is selected. We call our algorithm ‘‘Selected Loading’’ (SL). We note that SL is a pragmatic approach to loading for coded OFDM, which explores a (hopefully promising) subset of all possibilities for loading. The identification of the optimum loading for coded OFDM requires a full search and thus is computationally prohibitive. We also note that instead of minimizing BER we equally could minimize transmit power for a given BER by evaluating BER for a number of transmit power values.

SL is computationally more complex than conventional loading in that a number of loading algorithms and BER computations need to be executed. In terms of overhead for signaling selected constellations between transmitter and receiver there is no difference between SL and conventional bit-loading.

B. Adaptive Interleaving

Next, we consider adaptive interleaving. Different from bit-loading, the choice of interleaving has only an effect if coded transmission is considered, and thus interleaver optimization has received less attention than bit-loading in the literature. Recent references which address the problem of adaptive interleaving are [24], [25]. Here, we present three adaptive interleaving algorithms for BICM MIMO-OFDM using the proposed error-rate analysis. We note that adaptive interleaving can be employed on its own or in combination with bit-loading. The former case may be preferable since no changes in signal constellations and thus modulation and demodulation are necessary.

1) *Best Interleaver of a Set*: The first method is based on selecting the best interleaver among a set of interleavers, where the best interleaver is again determined using the general error-rate analysis derived earlier. When combining this adaptive interleaving method with bit-loading, the proposed scheme performs a search for both loading and interleaving for each channel realization. A pragmatic choice for this search is a two-step (greedy-type) approach, which in a first step selects the best interleaver for a non-loaded system, and in a second step selects the best loading for this given interleaver. There are a number of options for determining the set of candidate interleavers from which the “best” is chosen. In Section V, we will present results for both random sets and sets optimized for particular channel models.

2) *Iterative Interleaver Improvement*: The second adaptive interleaver algorithm starts from an initial interleaver and improves it by going through several iterations. Each iteration consists of the following steps:

- 1) Calculate $P_{i,\ell}(\mathbf{\Lambda}) = a_\ell \cdot \text{PEP}_{i,\ell}(\mathbf{\Lambda})$.
- 2) Find the error vector and starting position of the largest $P_{i,\ell}(\mathbf{\Lambda})$, which we denote as e_{max} and p_{max} , respectively.
- 3) Find the starting position of the smallest $P_{i,e_{max}}(\mathbf{\Lambda})$, which we denote as p_{min} .
- 4) Find the subcarriers that contain the error vector e_{max} at the starting position of p_{max} and store their gains in the vector \mathbf{g}_{max} .
- 5) Find the subcarriers that contain the error vector e_{max} at the starting position of p_{min} and store their gains in the vector \mathbf{g}_{min} .
- 6) Find the minimum of the vector \mathbf{g}_{max} and find the corresponding position of the interleaver which we denote as $index_{min}$.
- 7) Find the maximum of the vector \mathbf{g}_{min} and find the corresponding position of the interleaver which we denote as $index_{max}$.
- 8) Exchange the values of interleaver for $index_{min}$ and $index_{max}$.
- 9) Calculate PEP for the new interleaver.

We observe that after several iterations, the algorithm may oscillate, i.e., it may find a repeated set of e_{max} , p_{max} and p_{min} . In this situation, our algorithm is modified to find the next largest $P_{i,\ell}(\mathbf{\Lambda})$ until it finds a set of e_{max} , p_{max} and p_{min} that has not been used before. It is worthwhile to note that the PEP calculation in step 9 is fast, since the new interleaver is different from the old one in only two positions and, as a result, only a few PEPs need to be recalculated.

3) *Spatial Interleaving*: A special case of MIMO-SVD transmission occurs if N_T separate information streams are transmitted.² In this case, the MIMO-OFDM system is considered as N_T parallel SISO-OFDM systems in which the data of each information stream is transmitted over its specific SVD subcarrier. We propose spatial interleaving for these systems. In spatial interleaving, we first sort the singular values and then circularly shift them by one for each subcarrier. For example,

in a $N_T = 2, N_R = 2$ MIMO-SVD system, the SVD operation will result to two singular values: $\lambda_{i,1}, \lambda_{i,2}$ for $1 \leq i \leq N$. In the standard system, $\lambda_{i,1}$ is always greater than or equal to $\lambda_{i,2}$ and therefore the resulting channel for the first source is better than the second source. When we want to deploy spatial interleaving in this case, we should keep $\mathbf{\Lambda}_i, \mathbf{U}_i$ and \mathbf{V}_i for the odd-numbered tones and switch the position of $\lambda_{i,1}$ and $\lambda_{i,2}$ in $\mathbf{\Lambda}_i$ and change \mathbf{U}_i and \mathbf{V}_i correspondingly for even-numbered tones. This way we will have two links with almost similar quality. To evaluate the performance of these systems, each system should be analyzed separately, and the overall performance of the system is given by the average of these performances.

4) *Remarks*: As mentioned above, the idea of adaptive interleaving has been considered in [24], [25]. In [24], the interleaver is symbol-based rather than bit-based as in our proposal, and the interleaver selected for each channel realization is derived according to the channel gains of each subcarrier such that error bursts are broken. Parallel to our work, [25] has devised an adaptive bit-interleaving scheme, where the interleaver is designed based on the bit level capacities of an equivalent binary channel model. However, using capacity as a metric may not be accurate in practical systems, as it does not take the particular coding scheme into account. Interestingly, the adaptive bit interleaver of [25] would result in the adaptive symbol interleaver of [24] for 4-QAM with Gray labeling. This is because bit level capacities for both bits in 4-QAM are equal and therefore, the corresponding metrics of the algorithm of [25] are the scaled versions of the metrics of [24]. Finally, we note that the BER approximations for coded OFDM derived in [10] and [11] are not applicable for adaptive interleaving, since in both cases ideal interleaving is assumed.

C. Adaptive Coded Modulation

Optimization of bit-loading and adaptive interleaving entails a computational complexity which may be too high for certain applications. An alternative to selecting the “optimal” constellation for each subcarrier as well as the “optimal” interleaver for BICM-OFDM is to choose a coded modulation scheme (a code of a certain rate and a signal constellation of a certain size, combined via a pre-defined bit-interleaver) from a finite set of such schemes. Each of these coded modulation schemes provides different data rates, and using the devised BER and FER analysis, we select the coded modulation scheme that achieves the highest rate while not exceeding the desired target FER. If the FER constraint cannot be achieved by any coded modulation scheme, no data is transmitted. This adaptive coded modulation is, in terms of computational complexity, also particularly appealing, since the FER computation does not start from scratch but rather needs only to include the different channel realizations.

Adaptive coded modulation has also been considered in [11], where the authors select the best combination of code rate and constellation size based on a simplified BER expression. We found, however, that this expression does not yield tight approximations of the BER and thus is not well-suited for the purpose of adaptive coded modulation.

²Separate information streams per spatial layer are used in, e.g., 3GPP LTE systems.

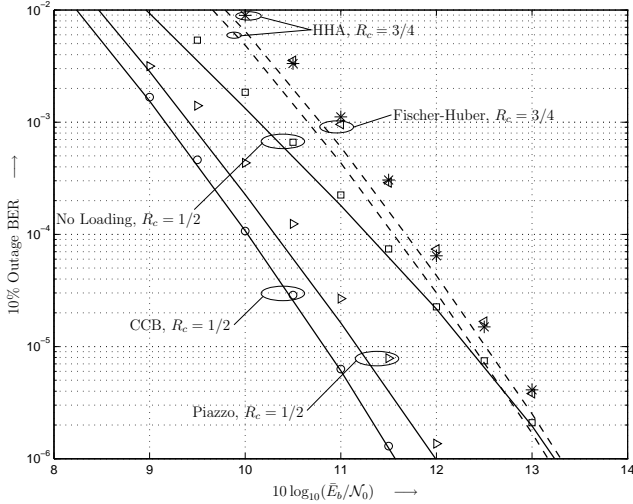


Fig. 1. 10% Outage BER versus $10 \log_{10}(\bar{E}_b/\mathcal{N}_0)$ from analysis (lines) and simulations (markers) for various combinations of code rates and loading algorithms. MB-OFDM system, UWB CM1 channel.

V. RESULTS

In this section, we present numerical results to illustrate the usefulness of the analysis presented in Section III and the performance of the adaptive schemes proposed in Section IV. Throughout this section, we allow $m_i \in \{0, \dots, 6\}$ coded bits per subcarrier, and employ loading schemes with an average $\bar{m} = 2$ coded bits per subcarrier unless noted otherwise. We consider the two OFDM systems described in Section II, namely MB-OFDM (Section II-B) and 802.11a/g with its MIMO extension (Section II-C).

A. Accuracy of BER Approximation

First, we illustrate the accuracy of the proposed BER approximation for coded and loaded OFDM. To this end, in Figure 1, we plot the 10% outage BER versus $10 \log_{10}(\bar{E}_b/\mathcal{N}_0)$ from analysis (lines) as well as the corresponding simulation results (markers) for various combinations of code rates and loading algorithms, for MB-OFDM over the UWB CM1 channel using a set of $N_c = 100$ channel realizations. (We note that the 10% outage BER is a common performance measure in UWB systems, cf. e.g. [2], [20].) We can see that the simulation results confirm the analysis for all considered code rates and loading algorithms, with a maximum difference of 0.3 dB between simulation and analysis at low BERs.

In Figure 2, the 10% outage BER versus $10 \log_{10}(\bar{E}_b/\mathcal{N}_0)$ from analysis (lines) as well as the corresponding simulation results (markers) for 802.11a/g WLAN are plotted for $N_T = 2$, $N_R = 2$ MIMO-SVD with different constellation sizes and code rates. We consider the case where there is the same information source for all antennas (“one source”) as well as the case where there is a separate information source for each SVD channel (“two sources”). It can be seen that again we have a very good match between simulation and analytical results which confirms the accuracy of our analytical expressions.

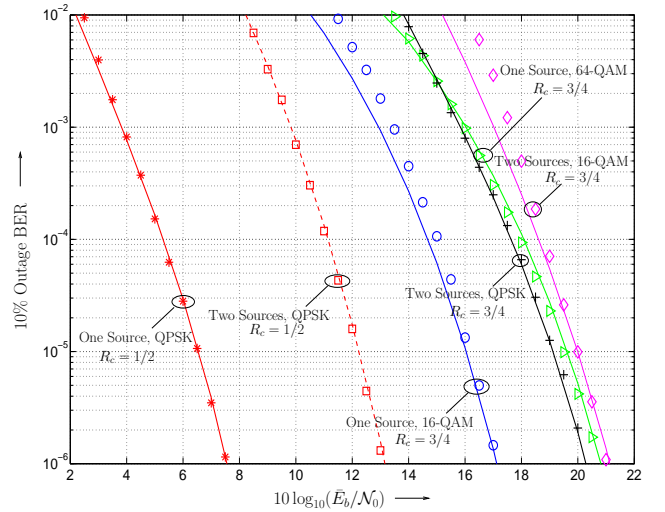


Fig. 2. 10% Outage BER versus $10 \log_{10}(\bar{E}_b/\mathcal{N}_0)$ from analysis (lines) and simulations (markers) for the MIMO-SVD system.

We note that obtaining the 10% outage BER via simulation is very time-consuming due to the need to simulate the system separately for each channel realization. On the other hand, the analysis can be performed quite quickly even for large sets of channel realizations.

In the following, we show BER results obtained from the analytical expressions unless noted otherwise.

B. Bit-Loading for Coded OFDM

Next, we show results for bit-loading for coded OFDM. Firstly, the MB-OFDM system with code rate $R_c = 1/2$ and transmission for the UWB CM1 is considered. Figure 3 shows the 10% outage BER versus $10 \log_{10}(\bar{E}_b/\mathcal{N}_0)$ for a number of popular loading algorithms, and the proposed SL algorithm. As a reference, the BER curve for coded OFDM without loading is also shown. We observe that for this system and channel model, decent gains of approximately 2 dB can be obtained by the application of loading. The Piazza and Fischer-Huber algorithms provide slightly smaller gains than the HHA and CCB algorithms. The proposed SL achieves the best performance, with modest additional gains over the conventional loading algorithms. Of course, this comes at the cost of the increased complexity required to perform the BER analysis for all loadings. Interestingly, the performance of sorted CCB is slightly better than those for HHA and CCB, which suggests use of sorted CCB also for coded OFDM due to its lower computational complexity [23]. The better performance of sorted CCB compared to CCB should not be alarming as neither of these algorithms is optimal and there is no guaranteed ranking when using them in combination with BICM. In order to reduce the computational complexity of SL, we also performed the SL using an error vector set of size $L = 1$, i.e., we only included the minimum distance error event in the analysis. The results obtained were identical to those in Figure 3. This suggests that reduced-complexity BER estimation with small error vector sets could be an attractive method for loading algorithms based on coded BER, such as SL.

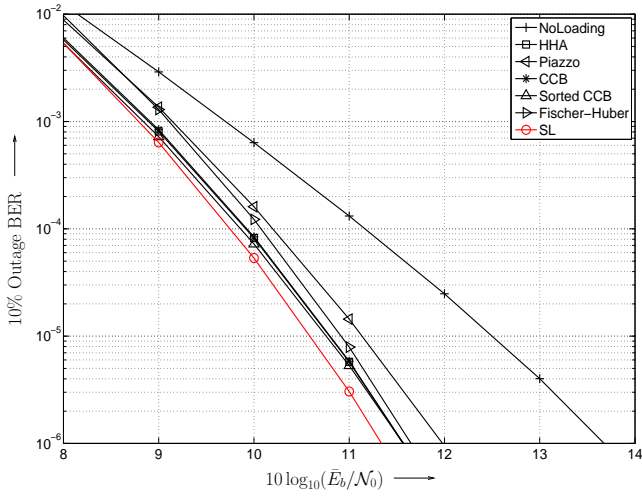


Fig. 3. 10% Outage BER versus $10 \log_{10}(\bar{E}_b/N_0)$ from analysis for various loading algorithms. MB-OFDM system with $R_c = 1/2$, UWB CM1 channel.

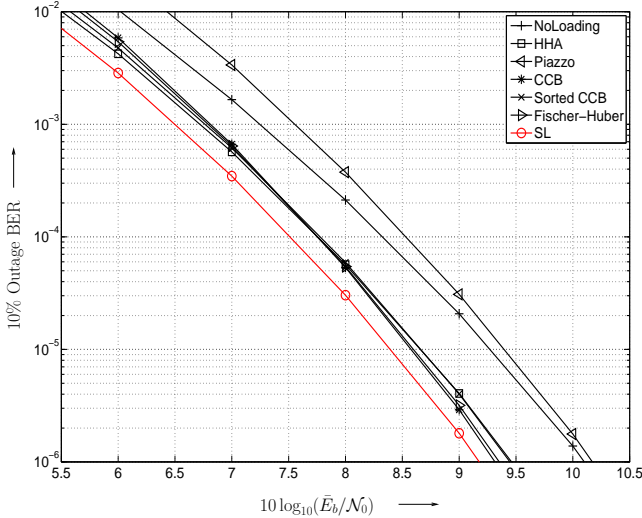


Fig. 4. 10% Outage BER versus $10 \log_{10}(\bar{E}_b/N_0)$ from analysis for various loading algorithms. 802.11a/g WLAN system with $R_c = 1/2$, channel $T_{rms} = 250$ ns.

Secondly, we consider the 802.11a/g WLAN system with code rate $R_c = 1/2$ and the channel model with RMS delay spread of $T_{rms} = 250$ ns. In Figure 4, we again plot the 10% outage BER versus $10 \log_{10}(\bar{E}_b/N_0)$ for the various loading algorithms. We observe relatively smaller gains due to loading than for the UWB scenario, and the Piazzo loading algorithm performs significantly worse than the other algorithms (see also Table II and the discussion below). Again, SL achieves the best performance. Furthermore, the sorted CCB algorithm achieves a performance very similar to those of HHA and CCB.

In order to see more comprehensive statistics for the comparison of the different loading schemes, Figure 5 shows the corresponding cumulative distributions of the loading gains $G = \text{SNR}_{\text{NL}} - \text{SNR}_{\text{Loading}}$ (NL: no loading) required to achieve a BER of 10^{-5} , for the MB-OFDM system with $R_c = 1/2$ over the UWB CM1 channel ($\text{SNR} \triangleq 10 \log_{10}(\bar{E}_b/N_0)$). Interestingly, we note that there is a small probability that the

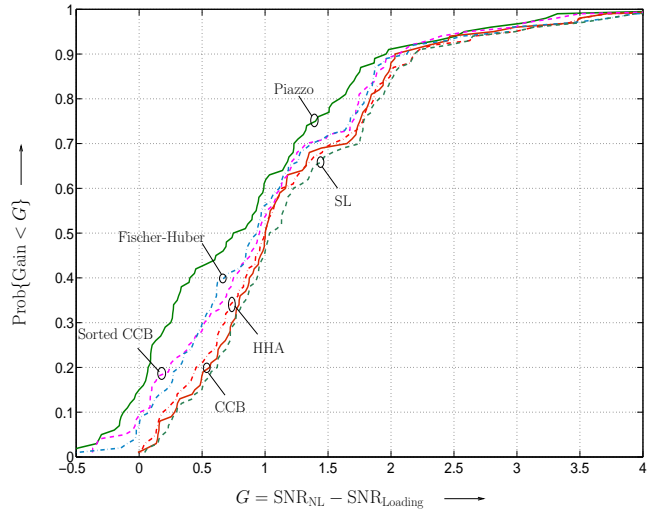


Fig. 5. Cumulative distribution function of loading gain $G = \text{SNR}_{\text{NL}} - \text{SNR}_{\text{Loading}}$ required for BER = 10^{-5} for different loading schemes (NL: no loading). MB-OFDM system with $R_c = 1/2$, UWB CM1 channel.

Piazzo, Fischer-Huber and Sorted CCB loadings will result in a performance loss (negative gains), while the CCB, HHA, and SL algorithms always provide a performance gain. We again note that HHA, CCB and Sorted CCB algorithms have similar performances. The SL always results in the highest loading gain. Finally, we note that gains of up to 4 dB can be expected from loading, while gains of at least 1 dB can be expected for 50% of channel realizations.

Finally, we consider the relative use of different loading schemes for the SL. Firstly, Table I lists the results for the case of MB-OFDM with $R_c = 1/2$ and $R_c = 3/4$ and the UWB CM1. Since calculating the HHA loading has a high computational complexity compared to the other algorithms, we list the relative use both including and excluding HHA (“w/ HHA” and “w/o HHA”, respectively). We note that for $R_c = 1/2$, CCB is the most-used algorithm, while for $R_c = 3/4$ the Fischer-Huber algorithm is often the best. The Piazzo algorithm is rarely the best loading for either code rate. By comparing the two code rates, we can see that the best loading algorithm is rate dependent, indicating that when deploying coded loaded OFDM systems, some consideration should be given to the loading-coding combination during system design. Secondly, Table II lists the relative use of different loading schemes in SL for the 802.11a/g system with $R_c = 1/2$ and different channel RMS delay spreads T_{rms} . Interestingly, we note that for small T_{rms} the best loading is often the same modulation for all subcarriers (no loading). This is a result of the lack of variation in subcarrier channel gains due to the small delay spread. As T_{rms} increases, the channel gains have more variation and thus there is increased gain from loading. We also note that the best loading is more varied for the WLAN case, indicating again that the choice of a loading algorithm for coded OFDM systems is system-dependent and should be carefully considered during system design.

TABLE II
RELATIVE USE OF DIFFERENT LOADING SCHEMES AS SELECTED LOADING. 802.11A/G, $R_c = 1/2$, OF (12), (13).

Loading	% Use ($T_{\text{rms}} = 50$ ns)		% Use ($T_{\text{rms}} = 100$ ns)		% Use ($T_{\text{rms}} = 250$ ns)	
	w/ HHA	w/o HHA	w/ HHA	w/o HHA	w/ HHA	w/o HHA
No Loading	90	91	57	60	18	19
HHA [3], [4]	2	—	8	—	19	—
CCB [5]	1	2	6	7	14	20
Sorted CCB [23]	6	6	25	28	39	48
Piazzo [6]	0	0	1	1	2	2
Fischer-Huber [7]	1	1	3	4	8	11

TABLE I
RELATIVE USE OF DIFFERENT LOADING SCHEMES AS SELECTED LOADING. MB-OFDM, UWB CM1 CHANNEL.

Loading	% Use ($R_c = 1/2$)		% Use ($R_c = 3/4$)	
	w/ HHA	w/o HHA	w/ HHA	w/o HHA
No Loading	0	0	0	0
HHA [3], [4]	42	—	86	—
CCB [5]	38	65	7	27
Sorted CCB [23]	7	16	3	10
Piazzo [6]	2	1	0	1
Fischer-Huber [7]	11	18	4	62

C. Adaptive Interleaving

In this section, we show results for the three proposed adaptive interleaving algorithms. We consider MB-OFDM with $R_c = 1/2$ for UWB CM1 and also MIMO IEEE 802.11a/g with $R_c = 1/2$.

1) *Impact of the Interleaver*: In Figure 6, we plot the BER versus $10 \log_{10}(\bar{E}_b/\mathcal{N}_0)$ for one specific channel realization from analysis (lines) as well as the corresponding simulation results (markers) when 3 different interleavers are used. In particular, the best and worst interleavers are chosen among 1000 randomly generated interleavers, as well as the interleaver prescribed by the MB-OFDM standard. We can see that interleaver has a great impact on the performance of the BICM systems. At the BER of 10^{-5} there is a difference of about 3.5 dB between the performance for the best and worst interleavers. Therefore, we conclude that analyses such as [10], [11], which consider the ideal interleaver, are not accurate in practical systems.

2) *Best Interleaver of a Set*: Next, we compare set-based adaptive interleaving using several different sets of interleavers. In particular, we compare

- always using the MB-OFDM standard interleaver;
- choosing the interleaver with the lowest BER from a set consisting of 1000 randomly generated bit-interleavers in addition to interleavers designed according to [24] with parameters $D = 2$ and $D = 4$ (we refer to this method as “best interleaver”); and
- choosing the interleaver with the lowest BER from a set of 10 bit-interleavers (the 9 best interleavers among random interleavers tested for another set of UWB CM1 channels, and the standard interleaver).

We also consider combined bit-loading and adaptive interleaving, where the interleaver is selected using option (c) above.

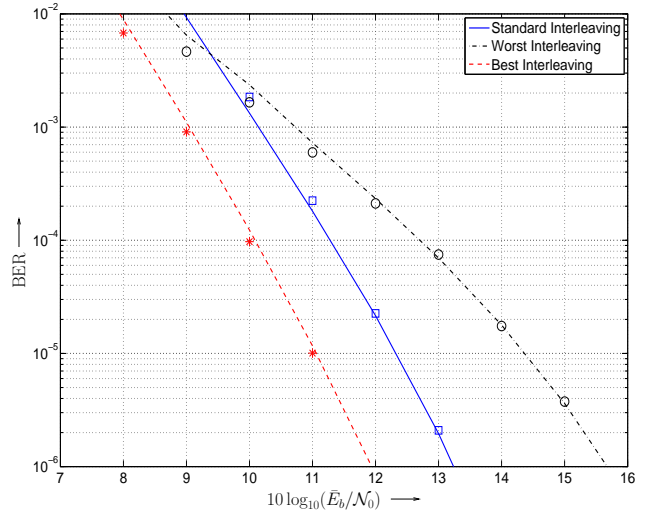


Fig. 6. Comparing different interleavers for one channel realization. MB-OFDM system with $R_c = 1/2$, UWB CM1 channel.

In Figure 7 we plot the average BER versus $10 \log_{10}(\bar{E}_b/\mathcal{N}_0)$ for the different adaptive interleaver schemes. The BER is averaged over $N_c = 2000$ channel realizations. As a reference, the BER for bit-loading with the fixed standard interleaver is also shown. We observe that adaptive interleaving without bit-loading results in a gain of about 1 dB for the considered scenario. If we restrict the search space to only 10 pre-selected interleavers, the gain diminishes, especially for lower error rates. We note that we obtained practically the same results if the interleavers were pre-selected based on a different UWB CM, e.g., CM3. Hence, we conclude the diversity of interleavers available, not the pre-selection, is critical for the performance gains with adaptive interleaving. Furthermore, it can be seen that the combination of adaptive interleaving and bit-loading has a small gain. This is different from the results reported in [25], where combining bit-loading and adaptive interleaving seems to result in a performance loss compared to plain adaptive interleaving.

Figure 8 provides further insight by showing the cumulative distribution of the adaptive interleaving gain $G = \text{SNR}_{\text{standard}} - \text{SNR}_{\text{adaptive}}$, where SNR_x is the SNR required to achieve a BER of 10^{-5} , for different adaptive interleaving schemes for $N_c = 1000$ channel realizations. In particular, the effect of the size of the set from which interleavers are selected is highlighted. It can be seen that there is no

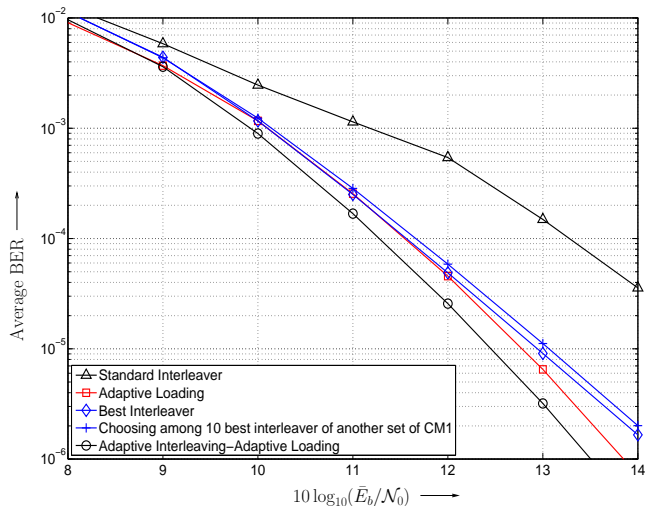


Fig. 7. Average BER for different set-based adaptive interleaver and adaptive loading schemes. MB-OFDM system with $R_c = 1/2$, UWB CM1 channel.

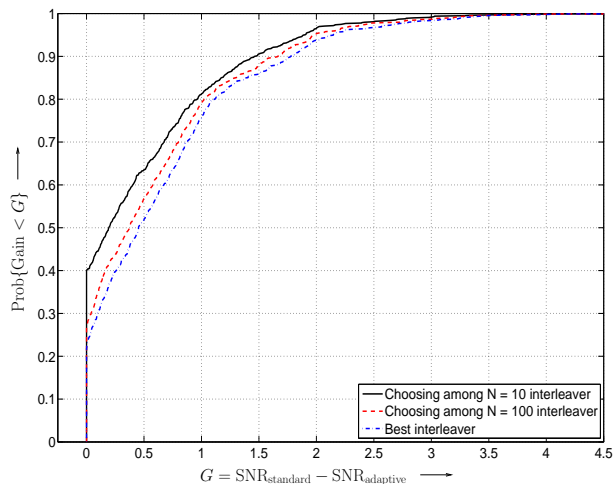


Fig. 8. Cumulative distribution function of interleaving gain $G = \text{SNR}_{\text{standard}} - \text{SNR}_{\text{adaptive}}$ required for $\text{BER} = 10^{-5}$ for different set-based adaptive interleaver schemes. MB-OFDM system with $R_c = 1/2$, UWB CM1 channel.

performance loss using our method. We also observe that gains of up to 4.5 dB can be expected from our proposed adaptive interleaving scheme.

3) *Iterative Interleaver Improvement*: The outage BER for our iterative interleaver improvement algorithm for 16-QAM is plotted in Figure 9, compared with the performance of the standard interleaver, symbol-based adaptive interleaving [24], and bit-based adaptive interleaving [25]. Our iterative algorithm starts with an initial interleaver from the bit-based adaptive algorithm. It can be seen that our algorithm will result in 0.5 dB performance gain over the bit-based algorithm, and approximately 1.3 dB gain over the symbol-based algorithm.

In Figure 10 the cumulative distribution of the gain $G = \text{SNR}_{\text{SF}} - \text{SNR}_{\text{our algorithm}}$ for our iterative interleaver improvement method is shown, where SNR_{SF} and $\text{SNR}_{\text{our algorithm}}$ are the SNRs required to achieve a BER of 10^{-5} for the bit-based adaptive algorithm of Stierstorfer and Fischer (SF) [25], and for our algorithm, respectively. It can

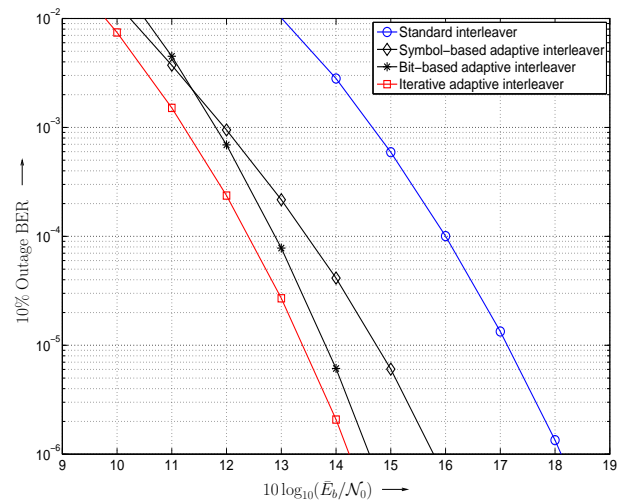


Fig. 9. 10% Outage BER for different adaptive interleaver schemes: symbol-based adaptive interleaver [24], bit-based adaptive interleaver [25], and our iterative adaptive interleaver algorithm. MB-OFDM system with $R_c = 1/2$, 16-QAM modulation, UWB CM1 channel.

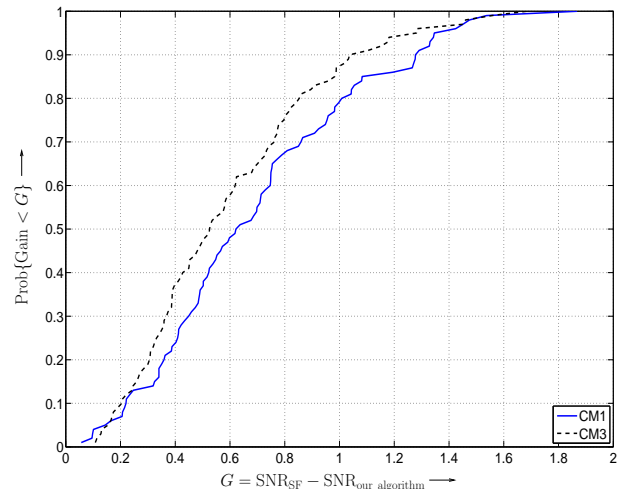


Fig. 10. Cumulative distribution function of the interleaving gain $G = \text{SNR}_{\text{SF}} - \text{SNR}_{\text{our algorithm}}$ required for $\text{BER} = 10^{-5}$ for our iterative adaptive interleaver versus bit-based adaptive interleaving (SF) [25]. MB-OFDM system with $R_c = 1/2$, 16-QAM modulation, UWB CM1 and CM3 channels.

be seen that gains of up to 2 dB can be expected from our method for both CM1 and CM3 channels.

4) *Spatial Interleaving*: The average BER for different adaptive interleaving techniques for 802.11a/g with 2 transmit and 2 receive antennas and two separate information sources are plotted in Figure 11. We can see that our proposed spatial interleaving results in about 5 dB performance gain. We can also combine spatial interleaving with other adaptive interleaving techniques. In this figure, we combine spatial interleaving with our set-based adaptive interleaving technique, where the best interleaver for each resulting channel is picked among the 10 best interleavers chosen for another set of channels. By doing so, we gain another 1.65 dB for the BER of 10^{-5} .

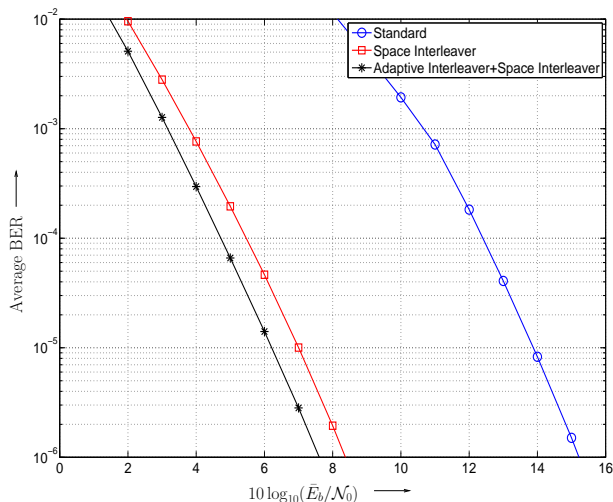


Fig. 11. Average BER for different adaptive interleaver schemes for MIMO-SVD. $R_c = 1/2$, 4-QAM modulation.

TABLE III

DIFFERENT CODE RATES AND MODULATIONS USED FOR THE SIMULATION RESULTS.

R_T	R_c	Modulation
1	1/2	4-QAM
1.33	2/3	4-QAM
1.5	3/4	4-QAM
2	1/2	16-QAM
2.67	2/3	16-QAM
3	3/4	16-QAM
3	1/2	64-QAM
4	2/3	64-QAM
4.5	3/4	64-QAM

D. Adaptive Coded Modulation

In this section, we show results for the proposed adaptive coded modulation scheme considering the 802.11a/g WLAN system with $T_{\text{rms}} = 250$ ns and $T_s = 50$ ns. We consider both the SISO system as well as 2×2 MIMO-SVD system with only one information source. The set of available code rates and modulations are shown in Table III, with total data rates from 1 bit/symbol to 4.5 bit/symbol. We call each combination of modulation and code rate a “mode”. For the results, we generate a set of 1000 channel realizations and for each channel realization, we select the appropriate mode using our error rate approximation, send the OFDM symbol over the channel, and decode it at the receiver. This allows us to measure the goodput (the successfully transmitted data rate), which has also been considered in [11]. A target frame error rate of 10^{-2} is adopted for both schemes.

The goodput versus $10 \log_{10}(\bar{E}/N_0)$ per subcarrier is plotted in Figure 12. The effect of different numbers of modes is analyzed in this figure. The system with 9 modes denotes the system which uses all the available code rates and constellation sizes. For 6 modes, $R_c = 2/3$ is not used and for 4 modes, 4-QAM with $R_c = 3/4$ and 64-QAM with $R_c = 1/2$ are also not used. It can be seen that using more modes will result in higher goodput because the system has more flexibility. However, the resultant gain is dependent on the SNR. This is

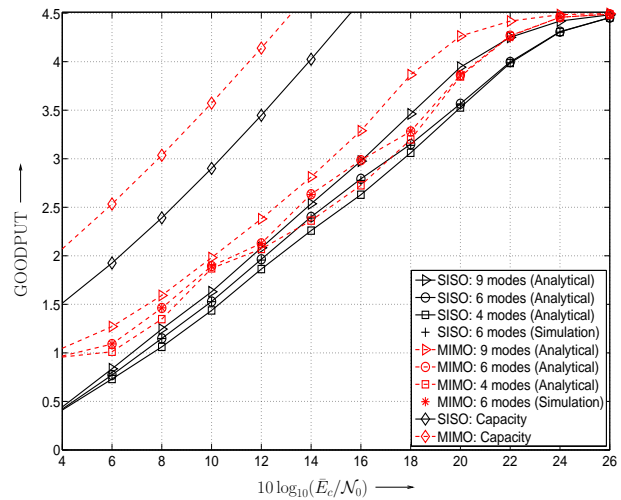


Fig. 12. Comparing the goodput for different adaptive coded modulation algorithms. 802.11a/g WLAN system, channel $T_{\text{rms}} = 250$ ns and $T_s = 50$ ns.

because in the low SNR region our method tends to select the lowest possible rate, thus having more modes does not help in this region. Simulation results for the 6 modes case are also plotted in this figure for both SISO and MIMO cases. It can be seen that analytical and simulation results perfectly match, again confirming the accuracy of the analytical results. Finally, we note that the gap to channel capacity for SISO and MIMO OFDM is consistently about 6 dB (using 9 modes), which is a promising result considering that convolutional codes are used.

VI. CONCLUSIONS

In this paper, we have developed a novel analytical method for BER and FER estimation of bit-loaded coded MIMO-OFDM systems operating over frequency-selective quasi-static channels with non-ideal interleaving. The presented numerical results illustrate that the proposed analysis technique provides an accurate estimation of the BER of loaded BICM-MIMO-OFDM systems. This allows for system performance analysis without resorting to lengthy simulations. We have put the analysis to use in three different applications, namely bit-loading, adaptive interleaving, and adaptive coded modulation. In the case of bit-loading, we have shown that the relative performance of bit-loading algorithms for coded OFDM is system-dependent, and thus some care should be given to the selection of loading algorithms for coded OFDM systems. The proposed Selected Loading guarantees the best performance, at a cost of somewhat higher complexity when performing the loading. Adaptive interleaving has been confirmed to be an interesting alternative and addition to bit-loading in coded OFDM. Finally, the application of the derived FER expressions to adaptive coded modulation algorithm leads to goodput close to the ultimate limit, while guaranteeing a certain target FER.

REFERENCES

- [1] IEEE 802.11, “Wireless LAN Medium Access Control (MAC) Physical Layer (PHY) Specifications, Amendment 1: High-Speed Physical Layer in the 5 GHz Band,” July 1999.

- [2] ECMA, "Standard ECMA-368: High Rate Ultra Wideband PHY and MAC Standard," Dec. 2005, [Online]: <http://www.ecma-international.org/publications/standards/Ecma-368.htm>.
- [3] J.A.C. Bingham, "Multicarrier Modulation for Data Transmission: An Idea Whose Time Has Come," *IEEE Commun. Mag.*, pp. 5–14, May 1990.
- [4] D. Hughes-Hartogs, "Ensemble Modem Structure for Imperfect Transmission Media," U.S. Patents Nos. 4,679,227 (July 1987), 4,731,816 (Mar. 1988), and 4,833,706 (May 1989).
- [5] P. S. Chow and J. M. Cioffi and J. A.C. Bingham, "A Practical Discrete Multitone Transceiver Loading Algorithm for Data Transmission over Spectrally Shaped Channels," *IEEE Trans. Commun.*, vol. 43, no. 2/3/4, pp. 773–775, Feb./Mar./Apr. 1995.
- [6] L. Piazzo, "Fast Algorithm for Power and Bit Allocation in OFDM Systems," *IEE Electronics Letters*, vol. 35, no. 25, pp. 2173–2174, Dec. 1999.
- [7] R. Fischer and J. Huber, "A New Loading Algorithm for Discrete Multitone Transmission," in *Proc. IEEE Global Telecommun. Conf. (GLOBECOM)*, London, Nov. 1996, pp. 724–728.
- [8] G. Caire, G. Taricco, and E. Biglieri, "Bit-Interleaved Coded Modulation," *IEEE Trans. Inform. Theory*, vol. 44, no. 3, pp. 927–946, May 1998.
- [9] J. G. Proakis, *Digital Communications*, 4th ed. New York: McGraw-Hill, 2001.
- [10] K.-B. Song and A. Ekbal and S.T. Chung and J. M. Cioffi, "Adaptive Modulation and Coding (AMC) for Bit-Interleaved Coded OFDM (BIC-OFDM)," *IEEE Trans. Wireless Commun.*, vol. 5, no. 7, pp. 1685–1694, July 2006.
- [11] C.K. Sung and S.-Y. Chung and J. Heo and I. Lee, "Adaptive Bit-Interleaved Coded OFDM With Reduced Feedback Information," *IEEE Trans. Commun.*, vol. 55, no. 9, pp. 1649–1655, Sept. 2007.
- [12] A. Martinez, A. Guillén i Fàbregas, and G. Caire, "Error Probability Analysis of Bit-Interleaved Coded Modulation," *IEEE Trans. Inform. Theory*, vol. 52, pp. 262–271, Jan. 2006.
- [13] S. Stiglmayr, M. Bossert, and E. Costa, "Adaptive Coding and Modulation in OFDM Systems using BICM and Rate-Compatible Punctured Codes," in *13th European Wireless Conference*, Paris, France, Apr. 2007.
- [14] C. Bockelmann, D. Wübben, and K.-D. Kammeyer, "Rate Enhancement of BICM-OFDM With Adaptive Coding and Modulation via a Bisection Approach," in *IEEE Intl. Workshop on Signal Processing Advances for Wireless Communications (SPAWC)*, Perugia, Italy, June 2009, pp. 658–662.
- [15] C. Mutti, D. Dahlhaus, T. Hunziker, and M. Foresti, "Bit and power loading procedures for OFDM systems with bit-interleaved coded modulation," in *Intl. Conf. on Telecommunications (ICT)*, Papeete, French Polynesia, Feb.-Mar. 2003, pp. 1422–1427.
- [16] S. Sand, C. Mensing, C. Mutti, and A. Wittneben, "Adaptive Bit Loading for BICM-OFDM with Square Lattice QAM Constellations," in *IEEE Intl. Conf. on Communications (ICC)*, Beijing, China, May 2008, pp. 3609 – 3615.
- [17] C. Snow, L. Lampe, and R. Schober, "Error Rate Analysis for Coded Multicarrier Systems over Quasi-Static Fading Channels," *IEEE Trans. Commun.*, vol. 55, no. 9, pp. 1736–1746, Sept. 2007.
- [18] M. Mohammadnia-Avval, C. Snow, and L. Lampe, "Error Rate Analysis for Bit-Loaded Coded OFDM," in *Proc. IEEE Wireless Communications and Networking Conference (WCNC)*, Las Vegas, USA, Mar.-Apr. 2008, pp. 4630–4635.
- [19] X. Liu and R. D. Wesel, "Profile optimal 8-QAM and 32-QAM constellations," in *Proc. 36th Annu. Allerton Conf. Communication, Control, and Computing*, 1998, pp. 136–145.
- [20] A. Batra, J. Balakrishnan, G. Aiello, J. Foerster, and A. Dabak, "Design of a Multiband OFDM System for Realistic UWB Channel Environments," *IEEE Trans. Microwave Theory Tech.*, vol. 52, no. 9, pp. 2123–2138, Sept. 2004.
- [21] A. F. Molisch, J. R. Foerster, and M. Pendergrass, "Channel Models for Ultrawideband Personal Area Networks," *IEEE Wireless Commun. Mag.*, pp. 14–21, Dec. 2003.
- [22] A. Saleh and R. Valenzuela, "A Statistical Model for Indoor Multipath Propagation," *IEEE J. Select. Areas Commun.*, vol. SAC-5, no. 2, pp. 128–137, Feb. 1987.
- [23] Z. Luo and H. Gao and Yuanan Liu, "Adaptive Transmission With Linear Computational Complexity in MIMO-OFDM Systems," *IEEE Trans. Commun.*, vol. 55, no. 10, pp. 1873–1877, Oct. 2007.
- [24] S.-W. Lei and V.K.N. Lau, "Performance Analysis of Adaptive Interleaving for OFDM Systems," *IEEE Trans. Veh. Technol.*, vol. 51, no. 3, pp. 435–444, May 2002.
- [25] C. Stierstorfer and R.F.H. Fischer, "Adaptive Interleaving for Bit-Interleaved Coded Modulation," in *Proc. 7th International ITG Conference on Source and Channel Coding*, Ulm, Germany, Jan. 2008.



Mohammad was a recipient of the Faculty of Applied Science Graduate Award from the University of British Columbia in 2008.

Mohammad Mohammadnia-Avval (S'05) was born in Mashhad, Iran in 1981. He received the B.S. degree from Amirkabir University of Technology, Tehran, Iran in 2003, and the M.Sc. degree from Sharif University of Technology, Tehran, Iran in 2005, both in electrical engineering. He is currently a Ph.D. candidate in the department of Electrical and Computer Engineering, University of British Columbia, Vancouver, Canada. His current research interests include analysis and design of MIMO and OFDM systems and adaptive communications. Mo-



Chris Snow was born in Winnipeg, Canada in 1979. He received the B.E.Sc. (Electrical Engineering) and B.Sc. (Computer Science) degrees from the University of Western Ontario in 2003, and the Ph.D. (Electrical Engineering) degree from the University of British Columbia in 2008. Since 2008 he has been with Research In Motion. His current research interests lie in the area of wireless communications, in particular in physical-layer and MAC-layer algorithms for cellular radio.



Lutz Lampe (M'02, SM'08) received the Diplom (Univ.) and the Ph.D. degrees in electrical engineering from the University of Erlangen, Germany, in 1998 and 2002, respectively. Since 2003 he has been with the Department of Electrical and Computer Engineering at the University of British Columbia, where he is currently an Associate Professor.

He is co-recipient of the Eurasp Signal Processing Journal Best Paper Award 2005 and the Best Paper Award at the 2006 IEEE International Conference on Ultra-Wideband (ICUWB). In 2003, he received the

Dissertation Award of the German Society of Information Techniques (ITG). He was awarded the UBC Killam Research Prize in 2008 and the Friedrich Wilhelm Bessel Research Award by the Alexander von Humboldt Foundation in 2009.

He is an Editor for the IEEE Transactions on Wireless Communications and the International Journal on Electronics and Communications (AEUE), and he has served as Associate Editor for the IEEE Transactions on Vehicular Technology from 2004 to 2008. He is Vice-Chair of the IEEE Communications Society Technical Committee on Power Line Communications. He was General Chair of the 2005 International Symposium on Power Line Communications and the 2009 IEEE International Conference on Ultra-Wideband.